

Dose-dependent cell growth in response to concentration modulated patterns of FGF-2 printed on fibrin

Eric D. Miller^a, Gregory W. Fisher^b, Lee E. Weiss^c, Lynn M. Walker^d, Phil G. Campbell^{e,*}

^aBiomedical Engineering, Carnegie Mellon University, Pittsburgh, PA 15213, USA

^bMolecular Biosensor and Imaging Center, Carnegie Mellon University, Pittsburgh, PA 15213, USA

^cThe Robotics Institute, Carnegie Mellon University, Pittsburgh, PA 15213, USA

^dDepartment of Chemical Engineering, Carnegie Mellon University, Pittsburgh, PA 15213, USA

^eInstitute for Complex Engineered Systems, Carnegie Mellon University, 5000 Forbes Ave, Pittsburgh, PA 15213, USA

Received 7 July 2005; accepted 31 October 2005

Available online 1 December 2005

Abstract

Immobilized patterns of unmodified fibroblast growth factor-2 (FGF-2), with varying surface concentrations, were inkjet printed onto physiologically relevant fibrin substrates. Printed patterns were characterized using iodinated FGF-2 to determine FGF-2 surface concentration and retention of FGF-2 binding *in vitro*. MG-63 cells were uniformly seeded onto patterned substrates. Cells were exposed to defined spatial FGF-2 surface concentrations of 1–22 pg/mm². Cell numbers were observed to increase in register with the printed FGF-2 patterns from an initial random uniform cell distribution across the patterned and non-patterned regions. Based on time-lapse image analysis, the primary organizational response of the cells was determined to be proliferation and not migration. Cell counts on and off the FGF-2 patterns over time demonstrated an increase in cell density up to a FGF-2 surface concentration of 14 pg/mm². Higher surface concentrations did not result in increased cell density. In addition, the cells on the FGF-2 patterns survived longer than the cells off patterns. Our inkjet printing approach permits the systematic study of cellular responses to defined spatial surface concentrations of immobilized growth factors.

© 2005 Published by Elsevier Ltd.

Keywords: Tissue engineering; Inkjet technology; Solid freeform fabrication; Growth factor; Printing technology; Biological patterning

1. Introduction

The work reported here demonstrates that two-dimensional concentration modulated patterns of fibroblast growth factor-2 (FGF-2), created with an inkjet printing methodology, direct cell proliferation in a dose-dependent manner up to a saturation surface concentration. This work is motivated by the need to study and apply concepts of biological patterning of endogenous hormones, including growth factors, which are known to play critical roles directing cell migration, proliferation, and differentiation during embryogenesis [1,2] and wound repair [3–5]. In nature, spatial patterning occurs via sequestration of growth factors in the interstitial space, which directly

affects temporal and spatial control by immobilizing growth factors at specific locations in the extracellular matrix (ECM) [6,7] or on the cell surface [8]. Immobilization permits local delivery of endogenous growth factors in physiological doses to induce cell mitogenesis and differentiation [9–13]. Thus, engineering the physical placement, concentration, and immobilization of exogenous growth factors in a physiologically relevant manner is important for biological research as well as a logical consideration for developing a tissue regeneration therapy.

Recent studies demonstrated that “solid-phase” growth factor delivery, a term which we use to refer to therapies that deliver growth factors immobilized to a scaffold, is biologically relevant and can be more effective than liquid-phase delivery with freely diffusible molecules [9–13]. Solid-phase delivery has been demonstrated using non-patterned uniform distributions of growth factors delivered within

*Corresponding author. Tel.: +1 412 268 4126; fax: +1 412 268 5229.

E-mail address: pcampbel@cs.cmu.edu (P.G. Campbell).

3D scaffolds. Solid-phase patterning of proteins has been accomplished in two dimensions using techniques such as photolithography [14,15], microcontact printing [16,17], and inkjet printing [18–22]. All of these methods, however, used chemical modification of the protein or substrate to ensure pattern persistence. In contrast, we recently reported on MG-63 cell behavioral responses to inkjet printed spatial patterns of FGF-2 immobilized via a native binding affinity on fibrin substrates as an initial investigation of cell behavioral responses to unmodified solid-phase growth factors patterned on native materials [22]. FGF-2 was selected as our model hormone because of its critical role in development and wound repair [23], its angiogenic [24] as well as osteogenic [25] properties, and its high-affinity binding for fibrin ($K_d \sim \text{nM}$) [26]. Fibrin was selected as our printing substrate because it serves as a provisional ECM during wound healing supports cell attachment and hormone sequestration [27]. The immobilized FGF-2 was shown to be biologically active, and the printed patterns persisted up to 10 days under cell culture conditions [22]. Cell numbers increased in register with concentration modulated printed patterns from an initial random uniform cell distribution across the patterned and non-patterned fibrin substrate. Patterned immobilized FGF-2, not cell attachment, directed cell organization because the fibrin substrate was homogeneous.

In our prior study, it was unclear if the cellular responses were due to proliferation, migration, or a combination of both [22]. In addition, printing fluorescently labeled FGF-2 illustrated that the patterns persisted *in vitro*; however, neither the surface concentration nor retention of the FGF-2 was determined. In the current study, we clarify the organizational response of the cells to the printed patterns and quantify the surface concentration of FGF-2 deposited and retained on the fibrin surface. We also further quantify the relationship between surface concentration of FGF-2 and cell density on the printed patterns.

2. Materials and methods

Unless otherwise indicated, all solvents used were reagent grade and were purchased from Fisher Scientific, Pittsburgh, PA.

2.1. Preparation of fibrin-coated printing substrates

Homogeneous fibrin films on glass slides were prepared as previously described [22]. Fibrinogen was obtained from Aventis Behring, King of Prussia, PA or American Diagnostica, Inc., Stamford, CT.

2.2. FGF-2 square array printing

Arrays of $0.750 \text{ mm} \times 0.750 \text{ mm}$ square FGF-2 patterns were printed onto the fibrin films using a custom inkjet printer that was described in detail previously [22]. In brief, the printer consists of a piezoelectric inkjet print head with a $30 \mu\text{m}$ nozzle (MicroFab, Inc., Plano, TX) mounted to xyz motion control stages (Aerotech, Inc., Pittsburgh, PA). The inkjet accuracy is $\pm 2 \mu\text{m}$. In contrast to conventional desktop printers, our system allows the user to have complete control over the jetting parameters. The drive waveform, firing rate, and dwell time for each

inkjet can be controlled independently to accommodate differences in biological “inks” (bioinks). The printing stage allows complete control over movement in the x , y , and z directions which permits freedom in depositing the bio-ink in any desired pattern. Custom software was used to program the stage and inkjet to create the patterns.

Prior to loading the FGF-2 bioink into the inkjet, the nozzle was immersed in $1 \mu\text{g/ml}$ bovine serum albumin (BSA) (Sigma Chemical Co., St. Louis, MO) for 5 minutes to prevent adsorption of the FGF-2 onto the glass nozzle. The nozzle was then emptied, rinsed 3 times with $0.2 \mu\text{m}$ filtered distilled deionized water, and loaded with $4 \mu\text{g/ml}$ recombinant human FGF-2, $17.2 \text{ kDa}/154$ amino acid form (Peprotech, Inc., Rocky Hill, NJ) in 10 mM sodium phosphate buffer, pH 7.4, to print the patterns. Prior to the initiation of printing FGF-2 patterns, we determined that physically jetting FGF-2 did not alter its bioactivity. Jetted and non-jetted FGF-2 were added as soluble components in a standard ^3H -thymidine incorporation (cell proliferation) assay with MG-63 cells. No difference in ^3H -thymidine incorporation into cellular DNA was observed between jetted and non-jetted FGF-2 confirming that jetting did not alter FGF-2 bioactivity (data not shown).

FGF-2 printed patterns consisted of an array of squares spaced 1.75 mm apart with each square containing a different number of overprints. The squares were 0.750 mm on each side with a center-to-center “spot” distance of $75 \mu\text{m}$. For the time-lapse experiments where the squares were imaged every 30 min, an array consisting of 4 squares of 2, 12, 22, and 32 overprints was printed. Fig. 1 illustrates the printing schematic for the array patterns. For the end-point experiments where the squares were imaged after 100 h in cell culture, arrays consisting of 9 squares were printed. Printed arrays contained squares with 2–34 overprints in increments of 4. In all of the patterns, a diamond-tipped pen was used to create 4 fiducial marks around each printed square so that it could be located later by microscopy.

After printing, the slides were placed in each well of a 12-well plate and sterilized in 70% ethanol for 10 min followed by 3 rinses with phosphate buffered saline (PBS), pH 7.4. The slides were incubated overnight at 37°C in minimal essential medium (Invitrogen Corp., Carlsbad, CA)

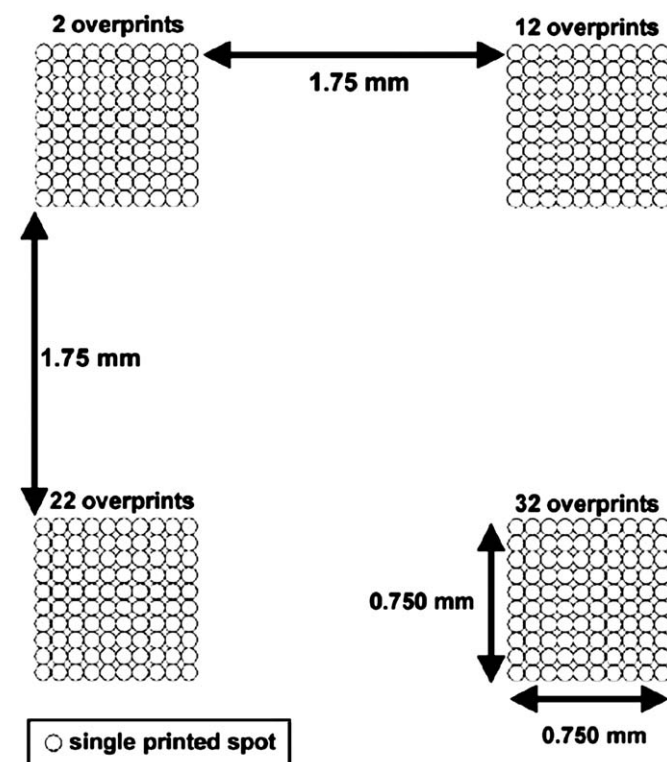


Fig. 1. Square array pattern design used for time-lapse experiments. Figure not drawn to scale.

supplemented with Ham's F-12 (MEM-F12) (Invitrogen Corp., Carlsbad, CA) and 1% penicillin/streptomycin (PS) (Invitrogen Corp., Carlsbad, CA) to remove any unbound FGF-2 from the fibrin surface. After rinsing, the slides were seeded with cells.

2.3. Cell culture

Human MG-63 "preosteoblastic" osteosarcoma cells (American Type Culture Collection, Manassa, VA) between passage 100 and 120 were used in all experiments and were cultured at standard conditions (37 °C, 5% CO₂) in MEM-F12, 10% calf serum (CS), and 1% PS. Cell suspensions for seeding the patterned slides were prepared by detaching the cells from the culture flasks with trypsin-EDTA, resuspending the cells in MEM-F12 with 10% CS, and centrifuging (4 °C, 50 g) and rinsing the cells 3 times with serum-free medium (MEM-F12 with 1% PS). Approximately, 40,000 cells in 2 ml of serum-free medium with 1 µg/ml aprotinin (Bayer Corp., Pittsburgh, PA) were added to each well of a 12-well plate containing a patterned slide.

For all experiments, the cells were allowed to attach for 3 h. The patterned slide was then removed from the plate, sterile silicon grease was used to fix the slide to the bottom of a 60 mm Petri dish, and the dish was filled with 8 ml of serum-free medium with 1 µg/ml aprotinin. For the time-lapse experiments, the dish with the patterned slide was placed in a custom microscope stage incubator. The incubator consisted of an aluminum chamber maintained at 37 °C using a stage heater (Brook Industries, NY) at the bottom of the chamber and an indium tin oxide-coated glass plate heater (Bioprotechs, Inc., Butler, PA) on the top of the chamber to prevent condensation from forming on the lid of the Petri dish. The chamber was sealed with silastic gaskets (Dow Corning, Midland, MI) and 5% CO₂ in air was introduced through a side port. Air flow was precisely regulated between 0.5 and 1.0 bar using a high precision flow valve, and the gas was humidified before entering the chamber. In addition, the stage incubator contained water reservoirs to maintain proper chamber humidity. Parallel cultures were maintained in a standard incubator to verify that the microscope stage incubator was functioning properly.

2.4. Image acquisition and processing

The microscope stage incubator was mounted on a Zeiss IM35 Axiovert microscope using a 5X, 0.15 N.A. phase 1 objective and phase optics (Carl Zeiss, Inc., Thornwood, NY) with a computer operated stage (Ludl Electronic Products Ltd., Hawthorne, NY). A ground glass diffuser was used to smooth out the bright field illumination. Time-lapse imaging of the patterns was automated using BDS-Image (Biological Detection Systems, Pittsburgh, PA) software and custom written software that runs within the BDS-image environment. The patterns (located using the marks scored on the slide after printing) were imaged every 30 min using a Photometrics C-250 cooled CCD camera, and the images were immediately processed by the software before the next image acquisition cycle. A total of 5 fields were imaged. Four of the fields contained the printed patterns, while the fifth field, adjacent to the 22 and 32 overprint squares, did not contain a printed pattern and served as a control. For the end-point experiments where arrays consisting of 9 squares were printed, the cell response was imaged only once at 100 h. The cell counting was performed as described previously [22].

2.5. Surface concentration of FGF-2

To quantify the binding and desorption of the growth factor from the fibrin surface, the FGF-2 was iodinated using a chloramine T method [28]. The fibrin-coated slides were "patterned" by placing a 1 µl drop of ¹²⁵I-FGF-2 onto the slide and allowing the drop to dry. The concentration of the ¹²⁵I-FGF-2 was selected so that the surface concentrations of the patterns created by the 2 methods would be comparable. The ¹²⁵I-FGF-2 blotted slides were placed in the wells of a 12-well plate and treated in the same manner as the regular patterned slides, including the 70% ethanol

immersion and 3 rinses in PBS. The quantity of ¹²⁵I-FGF-2 on each slide was counted after applying the 1 µl drop, after the 70% ethanol rinse, and after each rinse with PBS using a Cobra II auto-gamma counter (Perkin-Elmer). The slides were placed in serum-free MEM-alpha with 25 mM HEPES, 0.01% sodium azide, and 1% PS and stored at 37 °C. The amount of ¹²⁵I-FGF-2 on the slides was measured, and the medium was replaced every 24 h.

3. Results

3.1. FGF-2 patterning and retention

To verify the accuracy of the printing process, FGF-2 labeled with Cy3 dye (Cy3-FGF-2) was initially printed onto the fibrin-coated substrates. A fluorescent image of a printed Cy3-FGF-2 square is shown in Fig. 2. The printed FGF-2 square was 0.750 mm on each side and consisted of printed spots approximately 75 µm in diameter. The pattern was overprinted 20 times with a bioink consisting of 80 µg/ml unlabeled FGF-2 and 20 µg/ml Cy3-FGF-2. After printing, the slide was sterilized in 70% ethanol and rinsed 3 times with PBS before being seeded with cells. The image in Fig. 2 was acquired after 4 days in cell culture. Based on the appearance of the individual printed spots of the square, it is clear that the inkjet printing process precisely and reproducibly patterns the FGF-2 on the substrate. From the fluorescent image of this printed Cy3-FGF-2 pattern in cell culture, it appeared that the FGF-2 was retained *in vitro*, however, additional experiments were needed to quantify this observation.

To further investigate the desorption characteristics and to quantify the amount of FGF-2 physically adsorbed to the fibrin surface, retention experiments were performed with ¹²⁵I-FGF-2. For these experiments, 1 µl drops of ¹²⁵I-FGF-2 were deposited onto the fibrin films with a micropipette to create a well-defined surface concentration

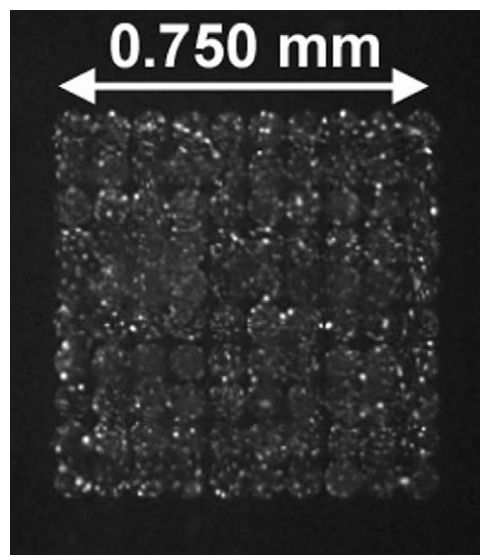


Fig. 2. Square pattern of FGF-2 printed onto a fibrin film imaged under Cy3 fluorescence after 4 days in cell culture. The pattern was printed using a bioink consisting of 80 µg/ml unlabeled FGF-2 and 20 µg/ml Cy3-FGF-2.

similar to those expected with the inkjet printing. Three different surface concentrations of ^{125}I -FGF-2 (35 ± 2 , 98 ± 2 , and $349 \pm 3 \text{ pg/mm}^2$) were applied to the fibrin-coated slides. The ^{125}I -FGF-2 blotted slides were treated in the same manner as the patterned slides, including the ethanol sterilization and 3 rinses in PBS. The slides were placed in serum-free medium and the amount of ^{125}I -FGF-2 present on the fibrin surface was measured over 9 days. The desorption profile for the 3 surface concentrations of ^{125}I -FGF-2 deposited on the slides is shown in Fig. 3. This figure shows a quantitative measure of FGF-2 surface concentration as a function of time over a 9-day period. The surface concentration at time zero (4 ± 0.1 , 10 ± 1 , and $37 \pm 2 \text{ pg/mm}^2$) indicates the amount of ^{125}I -FGF-2 retained on the slide after the ethanol sterilization and the 3 PBS rinses. Note that these values are significantly lower than the delivered concentration. Based on the highest dosage of ^{125}I -FGF-2 delivered, up to $20 \pm 1\%$ of the initial delivered ^{125}I -FGF-2 was lost in the ethanol sterilization. There was an additional $66 \pm 1\%$ loss of ^{125}I -FGF-2 after the first rinse in PBS. Subsequent washing in PBS resulted

in an additional $3 \pm 0.3\%$ and $0.5 \pm 0.1\%$ loss after the second and third rinses, respectively. Similar release rates were exhibited by the lower doses. In the first 24 h in serum-free media, approximately 25% of the ^{125}I -FGF-2 surface concentration at time zero was released from all of the blotted slides. After the initial 24 h media incubation, there was a much slower release of ^{125}I -FGF-2 from all of the blotted slides as indicated by the leveling off of the curves seen in Fig. 3. With the patterned slides, the cells were added to the substrate after the slides had been incubated for 24 h in serum-free media, as indicated by the dashed vertical line in Fig. 3. This result supports our prior FGF-2 retention experiments using Cy3-FGF-2 [22] and indicates that the cells seeded on the patterned slides experienced very little FGF-2 in the liquid phase and were primarily interacting with the FGF-2 adsorbed to the fibrin surface.

Table 1 illustrates the amount of ^{125}I -FGF-2 deposited initially onto the fibrin surface, the amount that was retained after the ethanol sterilization, PBS rinses, and 24 h medium soak, and the amount that remained bound after 9 days in serum-free media. The data indicate a linear relationship between the applied and the final FGF-2 surface concentrations up to the highest applied surface concentration, $349 \pm 3 \text{ pg/mm}^2$. Clearly, saturation of the FGF-2 binding sites on the fibrin surface was not attained in the concentration range tested. Since the surface concentration tested with the blotting ($35\text{--}349 \text{ pg/mm}^2$) was similar to the amount of FGF-2 delivered to the surface in the printed patterns (calculated to be from 20 to 320 pg/mm^2), we expect that the desorption of the FGF-2 from the patterns follows a trend similar to the experimental data shown in Fig. 3. These experimental results demonstrate that the cells on the printed patterns are interacting with a constant concentration of adsorbed FGF-2 and not soluble FGF-2 and that there is a direct linear relationship between the amount of FGF-2 that is applied to the fibrin surface and that which is available to the cells.

3.2. Cellular response to patterned FGF-2

After printing the square arrays of FGF-2, the patterns were seeded with cells and placed in the microscope stage

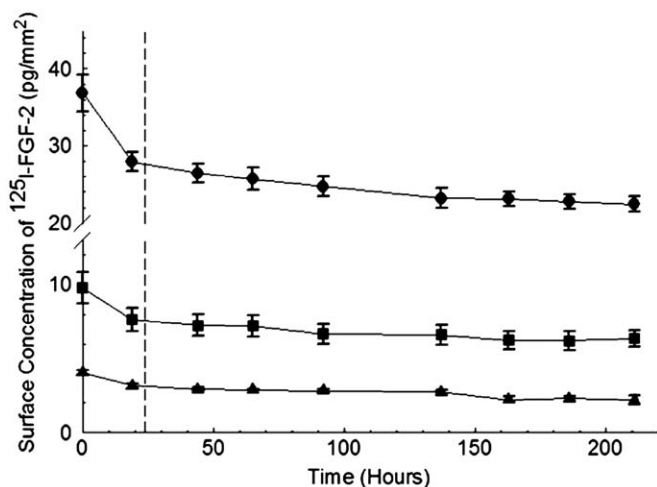


Fig. 3. Desorption profile of ^{125}I -FGF-2 from fibrin-coated surface over 9-day period. Three different concentrations of ^{125}I -FGF-2 were initially applied to each surface: $35 \pm 2 \text{ pg/mm}^2$ ▲, $98 \pm 2 \text{ pg/mm}^2$ ■, and $349 \pm 3 \text{ pg/mm}^2$ ●. Time zero represents the FGF-2 surface concentration after ethanol sterilization and PBS rinses. Each point represents mean \pm SEM of three different experiments.

Table 1
Surface concentration of ^{125}I -FGF-2 applied to fibrin film, amount retained after ethanol sterilization, 3 PBS rinses and 24 h incubation in medium, and amount retained after 9 days

Applied FGF-2 surface concentration (pg/mm^2)	FGF-2 surface concentration after sterilization, 3 PBS rinses, and 24 h medium soak (pg/mm^2)	Final FGF-2 surface concentration (pg/mm^2)
349 ± 3	28 ± 2	22 ± 1
98 ± 2	8 ± 1	6 ± 1
35 ± 2	3 ± 0.2	2 ± 0.3
Printed amount	Surface concentration at cell seeding	Surface concentration during cell incubation

Results represent mean \pm SEM of three different experiments.

incubator for time-lapse imaging of the cells on the patterns. As reported previously, a cellular response was observed in register with the printed patterns which demonstrated that inkjet bioprinted immobilized FGF-2 was biologically active [22]. Representative images demonstrating the response of the MG-63 cells to the printed patterns of FGF-2 after 61 and 176 hours in cell culture are shown in Fig. 4A and B, respectively. In this experiment, the cell density on the 4 different patterns was very similar after 61 h. The cells on the 12, 22, and 32 overprint patterns were more phase bright than the cells on the 2 overprint pattern and the surrounding off-pattern cells in each image field, indicating that they were not as firmly attached to the fibrin surface. This behavior was observed in many of the time-lapse movies where the cells on the patterns were generally more active and mobile than the off-pattern cells. The time-lapse movies also demonstrated that cell division off of the FGF-2 patterns was minimal compared to cell growth directly on the patterns. After 176 h, the increase in cell density on the 12, 22, and 32 overprint patterns was clearly visible, while it was not as obvious on the 2 overprint square. Upon inspection, there was a distinct difference in cell density between the 4 patterns after 176 h with the 2 overprint pattern having the least number of cells and the 32 overprint pattern having the highest cell number. At 176 h, the cells on the patterns were not as phase bright as at 61 h, cell division on the pattern had slowed down, and the cells appeared more spread out. After 8 or 9 days in cell culture, the cells surrounding the patterns generally had died and detached from the fibrin surface, while the on-pattern cells appeared healthy (images not shown). The cells on the patterns of FGF-2 survived longer than off-pattern cells and appeared to proliferate in register with the printed patterns in a dose-dependent manner.

Negative control patterns were also prepared by patterning both sodium phosphate buffer and BSA in sodium phosphate buffer on the fibrin films to demonstrate

that our results were specific to FGF-2. The slides were prepared as described and seeded with a uniform distribution of cells on the patterned and unpatterned regions of the substrate. The slides were imaged at 4 h, 3 and 7 days. No response was observed in register with any of the negative control patterns printed with the cell distribution remaining uniform on the substrate.

To quantitatively measure the response of the cells to the squares of different FGF-2 surface concentration, image processing techniques were used to count the cells on each printed pattern and the area in the image field immediately surrounding each printed pattern. Fig. 5A is a representative plot of the cell number on each square normalized by the initial cell number and area of the pattern versus time in hours. The cell numbers surrounding each pattern are also included on the plot as a baseline and are also shown in Fig. 5B. This figure is representative of many experiments that were performed with the same general trend in cell growth observed. Images and cell counts were obtained every 30 min in the experiment, however, for clarity only the data for every hour is shown in the plot. Time zero represents 4 h after the cells were initially seeded on the slides. The figure clearly illustrates that there was a drastic difference in cell growth between the on-pattern and off-pattern cells. Based on the overlap of the growth curves (Fig. 5A and B), the cells surrounding the FGF-2 patterns responded in a manner that was independent of the surface concentration of the printed FGF-2 square. The off-pattern cells displayed some minimal growth until approximately 125 h when the growth curve leveled off and started to drop indicating the onset of cell death. In contrast, all of the cells on the printed patterns divided rapidly for the first 60 h and continued to divide until about 180 h where the cell growth started to level off and cell death started to occur. As seen in the figure, the rate of cell growth was dose dependent on the surface concentration of FGF-2. The 2 overprint square had the slowest growth rate followed by the 12 overprint square and then the 22 and 32 overprint

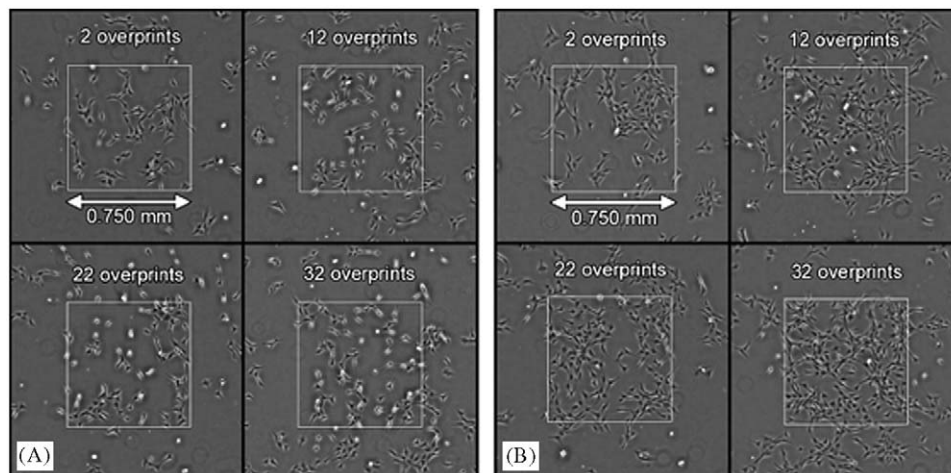


Fig. 4. Phase contrast images of MG-63 cell response to printed patterns of FGF-2 with 2, 12, 22, and 32 overprints on fibrin films. The patterns were imaged after 61 h (A) and 176 h (B) in cell culture. The location of the pattern is outlined with a square.

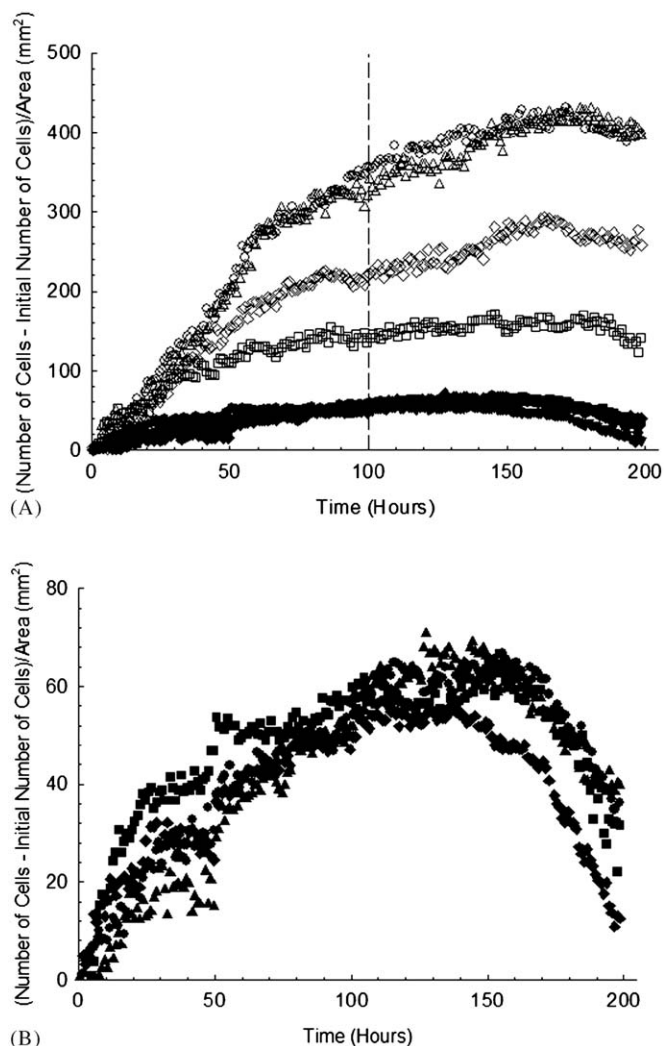


Fig. 5. Images of printed FGF-2 squares with a varying number of overprints were acquired every 30 min using phase contrast microscopy: (A) The images were processed and the cells both on the patterns and the cells off-pattern in the same image field were counted. The open symbols on the plot represent cells that are on the FGF-2 patterns: 2 overprints \square ; 12 overprints \diamond ; 22 overprints \circ ; 32 overprints \triangle . The closed symbols are cells that are in the same field but are surrounding the patterns: 2 overprints \blacksquare ; 12 overprints \blacklozenge ; 22 overprints \bullet ; 32 overprints \blacktriangle . (B) Expanded view of off-pattern cell counts.

squares which had a similar growth rate. Along with a trend in growth rate, there was clearly a relationship between the cell density and the surface concentration of FGF-2 based on the cell numbers at 180 h, the plateau region of each curve. The cell density on each pattern increased in register with the surface concentration of FGF-2 up to 22 overprints. At the higher doses of FGF-2, 22 and 32 overprints, the growth curves overlapped indicating that a level of saturation for the cells had been reached. Although a patterned response at 2 overprints was seldom clearly seen in the images, the cell counts indicate that there was still more cell division on the 2 overprints square than off-pattern. The results of this experiment illustrated that the cells on the FGF-2 patterns proliferated

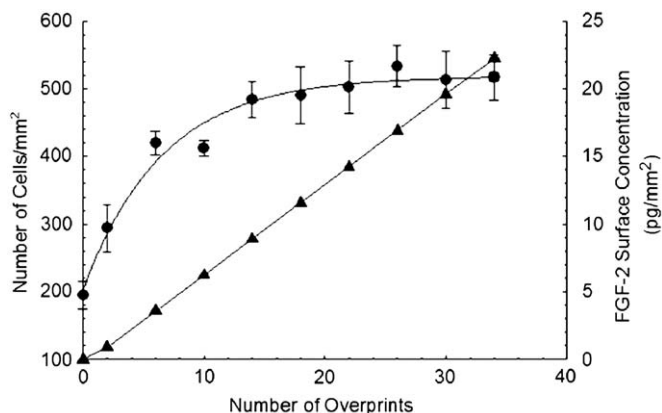


Fig. 6. A total of 3×3 square arrays of FGF-2 with varying numbers of overprints were printed and seeded with cells. The patterns were imaged after 100 h and the cells on each square were counted. Number of cells/mm² with each point representing mean \pm SEM of three different experiments \bullet ; final FGF-2 surface concentration of printed patterns determined indirectly from ¹²⁵I-FGF-2 desorption experiments \blacktriangle .

significantly more and were shown to inhibit cell death longer than the cells off-pattern. In addition, these results also demonstrate that cell density could be controlled by altering the surface concentration of FGF-2 up to a level of saturation.

To further clarify the relationship between cell density and surface concentration of FGF-2, experiments were performed where 9 square patterns with different surface concentrations were printed, seeded with cells, placed in a standard incubator, and then imaged after 100 h. This time point was selected because it was close to the plateau level of cell growth in many of the time-lapse experiments performed and it was well before the onset of cell death. This time point is indicated by the dashed vertical line in Fig. 5A. The results of this endpoint experiment are shown in Fig. 6. In agreement with the trend observed with the time-lapse result in Fig. 5, there was an increase in cell growth with increasing overprints until a level of saturation was achieved. These results further verified that inkjet printing can be used to vary the surface concentration of immobilized FGF-2 to control cell density and proliferation up to a level of saturation.

4. Discussion

4.1. FGF-2 patterning and retention

Many different patterning techniques, such as photolithography, microcontact printing, and inkjet printing have been used to create two-dimensional patterns of proteins. We chose to use inkjet printing for patterning because of its versatility. New patterns can easily be printed by altering a computer program in contrast to other methods where new stamps or photomasks are needed which require both additional time and costs. In addition, inkjet printing allows the surface concentration of the

printed proteins to be modulated by selective overprinting on the pattern and is extensible to creating 3D patterns [29]. One possible limitation of inkjet printing is its resolution. Since the printed drop size is limited by fluid mechanics, inkjet printing does not have the single micron resolution of other patterning methods. However, for cells that are approximately 100 μm when fully spread, tens-of-microns resolution is sufficient to influence cell behavior as demonstrated in this paper.

One issue with using native materials in our system is that desorption of some fraction of the delivered protein is expected. Therefore, we characterized the binding pharmacokinetics of the FGF-2 on the fibrin surface. To quantify the surface concentration and retention of FGF-2 bound to the fibrin surface, desorption experiments with ^{125}I -FGF-2 were performed using surface concentrations that fall within the range created by overprinting patterns. To determine the surface concentrations of the printed FGF-2 patterns, the in-flight volumes of the jetted droplets were calculated using images acquired with a high-speed motion capture system (Phantom V7, Vision Research, Wayne, NJ). The drop volume deposited with the printing parameters used to print all of the patterns was measured to be 14 ± 4 pl. Based on the amount of FGF-2 delivered to the surface in each printed drop, the deposited surface concentrations of the printed patterns could be determined. Two overprints corresponded to 20 pg/mm^2 , 12 overprints to 120 pg/mm^2 , 22 overprints to 220 pg/mm^2 , and 32 overprints to 320 pg/mm^2 . The results in Table 1 show that there was a linear relationship between the amount of ^{125}I -FGF-2 initially applied to the fibrin surface and the amount that was retained over 9 days. Based on this linear relationship, the final surface concentrations of each of the printed patterns can be determined indirectly and were calculated to be 1, 8, 14, and 21 pg/mm^2 for 2, 12, 22, and 32 overprints, respectively. These surface concentrations on the printed patterns were sufficient to elicit a biological response.

4.2. Cellular response to FGF-2 patterns

The desorption experiments with ^{125}I -FGF-2 (Table 1 and Fig. 3) and printing the Cy3-FGF-2 (Fig. 2) proved that our inkjet printing system could be used to reproducibly create solid-phase patterns of growth factors onto a biologically relevant surface. Previous studies have demonstrated that FGF-2 binds to fibrin with high affinity [26] while retaining its biological activity and that the binding actually increases its proliferative effects [12]. The results presented here support these observations by demonstrating that FGF-2 can be deposited on a fibrin surface with inkjet printing while retaining biological activity despite sterilization in ethanol [22].

Our results demonstrate that cell density can be controlled by altering the surface concentration of FGF-2. There was an observed increase in cell number with increasing overprints until a saturation point was reached

(Figs. 5–6). Another study has reported a similar trend in endothelial cells treated with increasing molar ratios of FGF-2 to fibrinogen [12]. Increasing cell proliferation was observed until a saturation point was reached where higher molar ratios of FGF-2 to fibrinogen no longer resulted in increased proliferation [12]. However, in the images presented in Fig. 4, the cells do not appear to be confluent and were not confluent in other experiments performed, as well. One explanation for this observation could be saturation of the available cell surface FGF-2 receptors for the cells present on the pattern.

Although there appeared to be a saturation level for the FGF-2 and cell density, all of the on-pattern growth curves exhibited similar trends. All of the curves had a very dramatic rise in cell number during the first 60 h in culture. The slopes of the curves leveled off in a dose-dependent manner with the 2 overprint curve reaching its plateau first at approximately 150 h and the 22, and 32 overprint curves leveling off later at about 180 h. The growth curves for the off-pattern cells were the same within experimental accuracy and reproducibility (Fig. 5B). In addition, cell counts on the control field which was adjacent to the 22 and 32 overprint squares followed the same growth trend as the off-pattern cells (data not shown). These observations strengthen the results of desorption experiments where minimal ^{125}I -FGF-2 was released from the surface after the initial 24 h incubation in serum-free media. The cells around the 32 overprints square were not proliferating more than the cells surrounding the square with 2 overprints. The initial growth in the off-pattern cells could be due to growth effects as a result of cell seeding or residual serum components surviving extensive rinse steps. The growth could also be due to the small amount of FGF-2 that was being released from the surface. However, even if all of the FGF-2 from the printed patterns was released in cell culture, the concentration of FGF-2 in solution would be 3 pg/ml which is too low to induce proliferation [12]. Cell death occurred after 125 h for the off-pattern cells as indicated by the decline in the growth curve while the on-pattern cells did not undergo apoptosis until 180 h. This observation is consistent with other studies where growth factor deprivation resulted in apoptosis of the cells [30]. The growth factor patterns prevented apoptosis of the cells and induced proliferation in a dose-dependent manner.

Time-lapse imaging of the patterns allowed for the cell organizational response to be determined. The patterns formed primarily by proliferation with no obvious directed cell migration to the patterns observed. This was consistent with the ^{125}I -FGF-2 desorption results which indicated that there was very little release of FGF-2 from the surface when the cells are present which would minimize the possibility of a liquid-phase concentration gradient of FGF-2 forming. This result coincides with the observations that the cell responses were formed by proliferation of cells that had landed on the FGF-2 squares during the initial cell seeding or migration of cells that were in the immediate vicinity of the squares and happened to encounter the

FGF-2 patterns by chance through random motion. However, it is most likely that only minimal migration of surrounding cells onto the patterns could occur since the cells that were on the FGF-2 patterns were generally more active than the off-pattern cells which were in a serum-deprived state and remained firmly attached to the fibrin surface. Additional data analysis of time-lapse movies will be needed to further clarify the role that cell migration and proliferation played in the patterned response observed. Experiments are currently being performed that focus solely on cell migration in response to solid-phase growth factor patterns including concentration gradients.

For all experiments reported here, we held the fibrin substrate concentration constant at 100 $\mu\text{g}/\text{ml}$ plated. Fibrin/fibrinogen binds cells through several integrins including $\alpha_v\beta_3$ which also interacts with the FGF-2 receptor 1 (FGFR1) to enhance the proliferation of endothelial cells treated with fibrin/fibrinogen bound FGF-2 [31]. FGF-2 has also been reported to complex directly to $\alpha_v\beta_3$ and influence endothelial cell attachment and spreading [32] but not proliferation or migration which only occurs via FGFR1 [33]. Therefore, the proliferation responses we observe with pg/mm^2 quantities of FGF-2 patterned upon fibrin may represent the synergistic response of FGF-2, FGFR-1, and $\alpha_v\beta_3$. Future experiments will determine the influence of the fibrin substrate concentration upon this interaction as well as the substitution or augmentation of fibrin with other ECM materials as printing substrates.

For these initial studies, we selected FGF-2 and fibrin as our model growth factor and printing substrate. However, this printing methodology is not limited to the combination of FGF-2, fibrin, and MG-63 cells. Other growth factors, including platelet derived growth factor-BB (PDGF-BB) and vascular endothelial growth factor (VEGF) also bind ECM proteins [9,34–36]. We have preliminary data demonstrating that we can also successfully pattern PDGF-BB and bone morphogenetic protein-2 (BMP-2) on fibrin and we have successfully used other ECM printing substrates such as fibronectin. We have also observed NIH3T3 and Swiss3T3 fibroblasts respond to solid-phase FGF-2 and PDGF-BB patterns. Along with being applicable for a variety of growth factors, substrate materials, and cell types, the versatility of inkjet printing allows for an essentially limitless design space. Patterns can be printed with the appropriate program and combinations of growth factors can be patterned by adding more print heads. Furthermore, while our current focus is on directing cellular proliferation and migration with 2D patterns, this solid-phase patterning methodology can be extended to create three-dimensional (3D) structures for use as a tissue engineering therapy. We are currently developing a second printer that is capable of creating 3D fibrin constructs containing spatial patterns of growth factors [37]. The spatial localization of growth factors in a physiologically relevant pattern, such as a concentration gradient, could amplify cell migration into the scaffold and promote

healing at the wound site. The printing system consists of a series of multiple, focused inkjet print heads which simultaneously deposit fibrinogen, thrombin, and FGF-2. The structures are built up layer-by-layer by the jetted droplets mixing and gelling on the substrate surface.

5. Conclusions

The results presented here demonstrate an inkjet printing method that uses native growth factors and a biologically relevant printing substrate. We show that our inkjet printing method can be used to control the surface concentration of FGF-2 and that cell density increases in register with the printed patterns up to a saturation level of approximately 22 overprints or a final surface concentration of 14 pg/mm^2 . Cell proliferation on patterns with lower FGF-2 surface concentrations were observed to plateau earlier than on the higher surface concentration squares. Desorption experiments using ^{125}I -FGF-2 demonstrated that the patterns were retained in vitro with less than a 30% loss of growth factor over 9 days. This indicates that initial cell growth off-pattern was not due to FGF-2 released from the surface. The cell counts on the area immediately surrounding each of the printed FGF-2 squares were identical within experimental error which demonstrated that the cells were not influenced by the concentration of the square that they were surrounding. However, the cells on the patterns of FGF-2 were observed to live longer than the cells surrounding the patterns in a dose-dependent manner. The results presented demonstrate how inkjet printing can be used to precisely and reproducibly deposit growth factors onto a biologically relevant surface to control cell proliferation.

Acknowledgments

This work was supported partially by the Office of Naval Research (Grant No. N000140110766), the National Science Foundation (Grants No. CTS-0210238 and DMI-9800565), the National Institutes of Health (Grant No. 1 R01 EB00 364-01), the Pennsylvania Infrastructure Technology Alliance (PITA) from the Pennsylvania Department of Community and Economic Development, the Health Resources and Services Administration (Grant No. 1C76 HF 00381-01), the Scaife Foundation, and the Philip and Marsha Dowd Engineering Seed Fund. We wish to thank Aventis Behring, L.L.C. (King of Prussia, PA) for their generous gift of lyophilized human fibrinogen and thrombin.

Competing interests statement: The authors declare that they have no competing financial interests.

References

- [1] Wolpert L. Positional information and the spatial pattern of cellular differentiation. *J Theor Biol* 1969;25:1–47.

- [2] Tickle C. Morphogen gradients in vertebrate limb development. *Semin Cell Dev Biol* 1999;10:345–51.
- [3] Singer AJ, Clark RA. Cutaneous wound healing. *N Engl J Med* 1999;341:738–46.
- [4] Gerstenfeld LC, Cullinane DM, Barnes GL, Graves DT, Einhorn TA. Fracture healing as a post-natal developmental process: molecular, spatial, and temporal aspects of its regulation. *J Cell Biochem* 2003;88:873–84.
- [5] Barnes GL, Kostenuik PJ, Gerstenfeld LC, Einhorn TA. Growth factor regulation of fracture repair. *J Bone Miner Res* 1999;14:1805–15.
- [6] Ruhrberg C, Gerhardt H, Golding M, Watson R, Ioannidou S, Fujisawa H, et al. Spatially restricted patterning cues provided by heparin-binding VEGF-A control blood vessel branching morphogenesis. *Genes Dev* 2002;16:2684–98.
- [7] Akeson AL, Greenberg JM, Cameron JE, Thompson FY, Brooks SK, Wiginton D, et al. Temporal and spatial regulation of VEGF-A controls vascular patterning in the embryonic lung. *Dev Biol* 2003;264:443–55.
- [8] Rifkin DB, Mazzieri R, Munger JS, Noguera I, Sung J. Proteolytic control of growth factor availability. *APMIS* 1999;107:80–5.
- [9] Sahni A, Francis CW. Vascular endothelial growth factor binds to fibrinogen and fibrin and stimulates endothelial cell proliferation. *Blood* 2000;96:3772–8.
- [10] Ehrbar M, Djonov VG, Schnell C, Tschanz SA, Martiny-Baron G, Schenk U, et al. Cell-demanded liberation of VEGF121 from fibrin implants induces local and controlled blood vessel growth. *Circ Res* 2004;94:1124–32.
- [11] Sahni A, Altland OD, Francis CW. FGF-2 but not FGF-1 binds fibrin and supports prolonged endothelial cell growth. *J Thromb Haemost* 2003;1:1304–10.
- [12] Sahni A, Sporn LA, Francis CW. Potentiation of endothelial cell proliferation by fibrin(ogen)-bound fibroblast growth factor-2. *J Biol Chem* 1999;274:14936–41.
- [13] Schmoekel HG, Weber FE, Schense JC, Gratz KW, Schawalter P, Hubbell JA. Bone repair with a form of BMP-2 engineered for incorporation into fibrin cell ingrowth matrices. *Biotechnol Bioeng* 2004;89:253–62.
- [14] Ito Y, Chen G, Imanishi Y. Micropatterned immobilization of epidermal growth factor to regulate cell function. *Bioconjug Chem* 1998;9:277–82.
- [15] Ito Y, Kondo S, Chen G, Imanishi Y. Patterned artificial juxtacrine stimulation of cells by covalently immobilized insulin. *FEBS Lett* 1997;403:159–62.
- [16] Bernard A, Delamarche E, Schmid H, Michel B, Bosshard H, Biebuyck H. Printing patterns of proteins. *Langmuir* 1998;14:2225–9.
- [17] Kane RS, Takayama S, Ostuni E, Ingber DE, Whitesides GM. Patterning proteins and cells using soft lithography. *Biomaterials* 1999;20:2363–76.
- [18] Sanjana NE, Fuller SB. A fast flexible ink-jet printing method for patterning dissociated neurons in culture. *J Neurosci Methods* 2004;136:151–63.
- [19] Turcu F, Tratsk-Nitz K, Thanos S, Schuhmann W, Heiduschka P. Ink-jet printing for micropattern generation of laminin for neuronal adhesion. *J Neurosci Methods* 2003;131:141–8.
- [20] Klebe RJ. Cytoscribing: a method for micropositioning cells and the construction of two- and three-dimensional synthetic tissues. *Exp Cell Res* 1988;179:362–73.
- [21] Watanabe K, Miyazaki T, Matsuda R. Growth factor array fabrication using a color ink jet printer. *Zoolog Sci* 2003;20:429–34.
- [22] Campbell PG, Miller ED, Fisher GW, Walker LM, Weiss LE. Engineered spatial patterns of FGF-2 immobilized on fibrin direct cell organization. *Biomaterials* 2005;26:6762–70.
- [23] Bikfalvi A, Klein S, Pintucci G, Rifkin DB. Biological roles of fibroblast growth factor-2. *Endocr Rev* 1997;18:26–45.
- [24] Bikfalvi A, Savona C, Perollet C, Javerzat S. New insights in the biology of fibroblast growth factor-2. *Angiogenesis* 1998;1:155–73.
- [25] Lieberman JR, Daluiski A, Einhorn TA. The role of growth factors in the repair of bone. *Biology and clinical applications. J Bone Joint Surg Am* 2002;84-A:1032–44.
- [26] Sahni A, Odrliin T, Francis CW. Binding of basic fibroblast growth factor to fibrinogen and fibrin. *J Biol Chem* 1998;273:7554–9.
- [27] Clark RA. Fibrin and wound healing. *Ann N Y Acad Sci* 2001;936:355–67.
- [28] Campbell PG, Skaar TC, Vega JR, Baumrucker CR. Secretion of insulin-like growth factor-I (IGF-I) and IGF-binding proteins from bovine mammary tissue in vitro. *J Endocrinol* 1991;128:219–28.
- [29] Calvert P. Inkjet printing for materials and devices. *Chem Mater* 2001;13:3299–305.
- [30] Araki S, Shimada Y, Kaji K, Hayashi H. Apoptosis of vascular endothelial cells by fibroblast growth factor deprivation. *Biochem Biophys Res Commun* 1990;168:1194–200.
- [31] Sahni A, Francis CW. Stimulation of endothelial cell proliferation by FGF-2 in the presence of fibrinogen requires $\alpha_v\beta_3$. *Blood* 2004;104:3635–41.
- [32] Rusnati M, Tanghetti E, Dell’Era P, Gualandris A, Presta M. $\alpha_v\beta_3$ integrin mediates the cell-adhesive capacity and biological activity of basic fibroblast growth factor (FGF-2) in cultured endothelial cells. *Mol Biol Cell* 1997;8:2449–61.
- [33] Tanghetti E, Ria R, Dell’Era P, Urbinati C, Rusnati M, Ennas MG, et al. Biological activity of substrate-bound basic fibroblast growth factor (FGF2): recruitment of FGF receptor-1 in endothelial cell adhesion contacts. *Oncogene* 2002;21:3889–97.
- [34] LaRochelle WJ, May-Siroff M, Robbins KC, Aaronson SA. A novel mechanism regulating growth factor association with the cell surface: identification of a PDGF retention domain. *Genes Dev* 1991;5:1191–9.
- [35] Raines EW, Lane TF, Iruela-Arispe ML, Ross R, Sage EH. The extracellular glycoprotein SPARC interacts with platelet-derived growth factor (PDGF)-AB and -BB and inhibits the binding of PDGF to its receptors. *Proc Natl Acad Sci USA* 1992;89:1281–5.
- [36] Park JE, Keller GA, Ferrara N. The vascular endothelial growth factor (VEGF) isoforms: differential deposition into the subepithelial extracellular matrix and bioactivity of extracellular matrix-bound VEGF. *Mol Biol Cell* 1993;4:1317–26.
- [37] Weiss LE, Amon C, Finger S, Miller ED, Romero D, Verdinelli I, et al. A Bayesian modeling approach to computer-aided experimental design of heterogeneous matrices for tissue engineering applications. *Computer-Aided Des* 2005;37:1127–39.